Communications in **M**athematical **A**nalysis
Volume 15, Number 2, pp. 76–102 (2013) www.math-res-pub.org/cma
ISSN 1938-9787

WELL-POSEDNESS OF A LINEAR SPATIO-TEMPORAL MODEL OF THE JAK2/STAT5 SIGNALING PATHWAY

E. FRIEDMANN[*]
Department of Applied Mathematics
University Heidelberg
Im Neuenheimer Feld 293
69120 Heidelberg, Germany

R. NEUMANN[†]
Interdisciplinary Center for Scientific Computing (IWR)
University Heidelberg
Im Neuenheimer Feld 368
69120 Heidelberg, Germany

R. RANNACHER[‡]
Department of Applied Mathematics
University Heidelberg
Im Neuenheimer Feld 293
69120 Heidelberg, Germany

(Communicated by Irena Lasiecka)

Abstract

Cellular geometries can vary significantly, how they influence signaling remains largely unknown. In this article, we describe a new model of the most extensively studied signal transduction pathways, the Janus kinase (JAK)/signal transducer and activator of transcription (STAT) pathway based on a mixed system of *linear* differential equations (PDEs + ODEs) coupled by Robin boundary conditions. This model was introduced to analyze the influence of the cell shape on the regulatory response to the activated pathway. In this article, we present an analysis of the well-posedness of the resulting system, i.e., the existence of a unique solution, its non-negativity, boundedness and Lyapunov stability. As by-product, we show the well-posedness and convergence of a suitable discretization of this model providing the basis for its reliable numerical simulation.

[*]E-mail address: friedmann@iwr.uni-heidelberg.de
[†]E-mail address: rebecca.neumann@iwr.uni-heidelberg.de
[‡]E-mail address: rannacher@iwr.uni-heidelberg.de

AMS Subject Classification: 35K57, 65M06, 65M12, 92C37, 92C40.

Keywords: Cell biology, signal transduction, reaction-diffusion problems, mixed PDE-ODE systems, well-posedness.

1 Introduction

In multicellular organisms communication between cells is frequently mediated by signal molecules secreted to the extracellular space which bind to cell surface receptors. The signal has to be transmitted from the extracellular domain of the cell surface receptors to the nucleus and thereby regulates gene expression.

How transport from the site of signal transducer and activator of transcription (STAT) phosphorylation at the plasma membrane to the site of action in the nucleus is mediated is still unclear. Whether STATs freely diffuse through the cytoplasm to reach the nuclear envelope or are actively transported along the cytoskeleton remains a matter of debate. Moreover, it is not known whether STATs can in addition be phosphorylated by membrane-bound kinases on endosomes present in the cytosol. This would reduce the distance between the site of phosphorylation and nuclear envelope. To answer these questions and to analyze the influence of the cell shape on the regulatory response to the activated pathway, a new model was introduced which takes the geometry of the cell into account. The key components of the pathway are modeled with a system of ordinary differential equations (ODEs) to estimate the parameters that can not be measured experimentally. The ODE model is then enlarged to include the transport of STAT5 through the cytoplasm, which is modeled by a heterogeneous reaction-diffusion process. A mixed system of differential equations (PDEs + ODEs) coupled by linear, time-dependent Robin boundary conditions is obtained, which is analyzed upon well-posedness, i. e., existence of a unique solution, its non-negativity, boundedness and Lyapunov stability. For this analysis, we employ an "energy technique" using the Banach fixed-point theorem rather than the abstract semigroup approach in order to cover general *non-autonomous* settings and also to prepare for an extension to more realistic *nonlinear* models. This will be the subject of a forthcoming paper. As by-product, we also obtain the well-posedness and convergence of a suitable discretization of this model yielding the basis for its reliable numerical simulation. Such a simulation is carried out using the in-house finite element package Gascoigne [10].

2 Biological Processes

One of the most extensively studied signal transduction pathways is the JAK/STAT pathway (see Pfeifer et al. [19]). Several members of the signal transducer and activator of transcription (STAT) protein family have been implicated in various cancers. Briefly, after binding of ligand to the receptor two receptor associated Janus kinases (JAK) transphosphorylate each other and subsequently tyrosine phosphorylate the cytoplasmic domain of the receptor. STAT proteins can then bind to the phospho-tyrosine residues via their SH2 domains and are phosphorylated by JAK. Phosphorylated STATs dissociate from the receptor, dimerize, move to the nucleus and regulate transcription of target genes. After gene transcription, the phosphorylated STATs are deactivated and exported back to the cytoplasm. Meanwhile

STATs are permanently imported and exported from the cytoplasm to the nucleus. The kinetics of these processes is given through the following reactions:

$$2(\mathrm{pJAK} + (\mathrm{STAT})) \xrightarrow{r_{\mathrm{act}}} (\mathrm{pSTAT}_{\mathrm{cyt}})_2 \xrightarrow{r_{\mathrm{imp2}}} (\mathrm{pSTAT}_{\mathrm{nuc}})_2$$
$$(\mathrm{pSTAT}_{\mathrm{nuc}})_2 \xrightarrow{\tilde{r}_{\mathrm{delay}}} 2(\mathrm{STAT}_{\mathrm{nuc}}) \xrightarrow{r_{\mathrm{exp}}} 2(\mathrm{STAT}_{\mathrm{cyt}}) \xrightarrow{r_{\mathrm{imp}}} 2(\mathrm{STAT}_{\mathrm{nuc}})$$

The model resulting from the kinetics is relaxed by a fixed sojourn time $\tilde{r}_{\mathrm{delay}}$ for STAT in the nucleus. It takes into account the processes in the nucleus like gene expression and deactivation, which are not the focus of this paper. The introduction of a distribution of the delay in four reactions improved the description of the experimental data significantly (see Timmer et al. [24]):

$$(\mathrm{pSTAT}_{\mathrm{nuc}})_2 \xrightarrow{r_{\mathrm{delay}}} (\mathrm{pSTAT}_{1\mathrm{nuc}})_2 \xrightarrow{r_{\mathrm{delay}}} (\mathrm{pSTAT}_{2\mathrm{nuc}})_2 \xrightarrow{r_{\mathrm{delay}}} (\mathrm{pSTAT}_{3\mathrm{nuc}})_2$$
$$(\mathrm{pSTAT}_{3\mathrm{nuc}})_2 \xrightarrow{r_{\mathrm{delay}}} (\mathrm{pSTAT}_{4\mathrm{nuc}})_2 \xrightarrow{r_{\mathrm{delay}}} 2(\mathrm{STAT}_{\mathrm{nuc}}).$$

2.1 Biological Data

A major limitation in systems biology often remains the lack of sufficient high-quality quantitative data for different variables of investigated systems. To overcome this constraint, we have based our mathematical modeling on experimental data acquired by different experimental techniques (described in Friedmann et al. [9]), all generating quantitative data of high quality. Our collaborators, the group of U. Klingmüller (Systems Biology of Signal Transduction, German Cancer Research Center, DKFZ Heidelberg) provides us with quantitative measurements of activation, localization and transport dynamics of several components of the JAK2/STAT5 pathway by immunoblotting and fluorescence microscopy (time lapse imaging, FRAP, FCS) in a NIH-3T3 fibroblast model system presented in Swameye et al. [23] and Pfeifer et al. [19] as well as in CFU-E cells communicated in Bachmann [3]. Nevertheless, the restrictions of each method have to be assessed carefully to avoid misinterpretations of data. In addition, it is advisable to establish standard procedures for cell culture, sample preparation and experimental setup to guarantee comparable results (see Schilling et al. [20, 21]).

3 Model Formulation

As mentioned above the key components of the pathway are modeled with a system of ordinary differential equations (ODEs), which is supplemented by a heterogenous reaction-diffusion model (PDEs) for the transport of STAT through the cytoplasm. This mixed system of *linear* differential equations (PDEs + ODEs) is coupled by likewise linear, but *time-dependent* Robin boundary conditions. In comparison to Swameye et al. [23], we focus on the dimeric description of the STAT molecules in the model, which results in a simplified *linear* model without being restrictive. We consider also a simplified receptor module. The binding of the ligand Epo to the extracellular part of the receptor, which leads to activation by phosphorylation of the JAK at intracellular cytoplasmic domain of the receptor, does not need to be modeled in detail. This is due to the possibility of measuring the phosphorylation function pJAK(t), the evolution in time of the activated cytoplasmic domain of the receptor.

3.1 An ODE Model

Models which describe the interaction between two domains, here the molecule exchange between the cytoplasm and the nucleus, are called two-compartment models. In such models the volume of the compartments play a crucial role in the equations.

We denote by u_0 the concentration of unphosphorylated STAT5 and by u_1 that of phosphorylated STAT5 in the cytoplasm, while u_2 denotes the concentration of unphosphorylated STAT5 and u_3 that of phosphorylated STAT5 in the nucleus, respectively. The variables $u_4, ..., u_7$ are introduced to describe the processes in the nucleus by linear delay equations, they are so-called "fictitious concentrations". The model for determining the state vector $u(t) = (u_0(t), \dots, u_7(t))$ looks as follows:

$$\nu_{\text{cyt}}\, u_0'(t) = -r_{\text{act}}\text{pJAK}(t)u_0(t) - r_{\text{imp}}u_0(t) + r_{\text{exp}}u_2(t), \tag{3.1}$$

$$\nu_{\text{cyt}}\, u_1'(t) = -r_{\text{imp2}}u_1(t) + r_{\text{act}}\text{pJAK}(t)u_0(t), \tag{3.2}$$

$$\nu_{\text{nuc}}\, u_2'(t) = -r_{\text{exp}}u_2(t) + r_{\text{imp}}u_0(t) + r_{\text{delay}}u_7(t), \tag{3.3}$$

$$\nu_{\text{nuc}}\, u_3'(t) = -r_{\text{delay}}u_3(t) + r_{\text{imp2}}u_1(t), \tag{3.4}$$

$$\nu_{\text{nuc}}\, u_i'(t) = -r_{\text{delay}}u_i(t) + r_{\text{delay}}u_{i-1}(t), \quad i = 4,5,6,7. \tag{3.5}$$

Summing all these equations, we see that the quantity

$$\sigma(u) := \nu_{\text{cyt}}(u_0 + u_1) + \nu_{\text{nuc}}(u_2 + u_3 + u_4 + u_5 + u_6 + u_7) \tag{3.6}$$

is conserved in time as required for physical reasons. This model was considered for two different cell types: a spherical-shaped CFU-E and a NIH3T3 fibroblast cell. We have two sets of parameters, one for each cell type. The initial values are

$$u_1(0) = u_3(0) = u_4(0) = u_5(0) = u_6(0) = u_7(0) = 0 \tag{3.7}$$

$$\text{CFU-E:} \quad u_0(0) = 50\ \text{mol}/\mu\text{m}^3, \quad u_2(0) = 18\ \text{mol}/\mu\text{m}^3 \tag{3.8}$$

$$\text{NIH3T3:} \quad u_0(0) = 16\ \text{mol}/\mu\text{m}^3, \quad u_2(0) = 20\ \text{mol}/\mu\text{m}^3, \tag{3.9}$$

where the number of molecules (mol) per compartment was determined using a combination of immunoprecipitation and immunoblotting as described in Friedmann et al. [9].

The determination of the parameters in the above model is a delicate matter. For illustration, we briefly describe the basis of the choices made in our simulations. The parameters ν_{cyt} and ν_{nuc}, which represent the average volume of the cytoplasm and nucleus were measured by transmitted light microscopy. We use the values $\nu_{\text{cyt}} = 429\ \mu\text{m}^3$, $\nu_{\text{nuc}} = 268\ \mu\text{m}^3$ for the CFU-E cell, and $\nu_{\text{cyt}} = 1758\ \mu\text{m}^3$, $\nu_{\text{nuc}} = 366\ \mu\text{m}^3$ for the NIH3T3 cell. The nuclear import and export rates r_{imp} and r_{exp} can be measured only for the unphosphorylated STAT in NIH3T3 cells by FRAP experiments. The import rate of the unphosphorylated STAT in the CFU-E cells is assumed to be approximately the same as in the NIH3T3 cells, so that the same value is used for both cell types in our model. Another input function in this model is the phosphorylation function pJAK(t). Its time distribution is given in form of discrete measurements, which are smoothly interpolated by splines. We assume that after some initial phase $[0, T]$ the function pJAK(t) becomes constant in time, i. e., pJAK(t) = pJAK for $t \geq T$. Further, to get the right amount of molecules, we assume that at the plasma membrane the number of JAK molecules is equal to the number of EpoR molecules.

parameter	unit	CFU-E cell	NIH-3T3 cell
r_{act}	min^{-1}	11	187
r_{imp}	min^{-1}	39	242
r_{imp2}	min^{-1}	58	1010
r_{exp}	min^{-1}	265	174.93
r_{delay}	min^{-1}	225	194.31
v_{cyt}	μm^3	429	1758
v_{nuc}	μm^3	268	323
pJAK(t)	-	[0,4.5]	[0,2.5]

Table 1. Parameters for the two different cell types.

With the system (3.1) - (3.5) parameter estimation has been performed using the software PottersWheel (see Maiwald & Timmer [17] and Friedmann et al. [9]). This tool has been developed for data-based modeling of partially observed and noisy systems like signal transduction pathways, i. e., for determining the unknown parameters, which are different in the different cell lines: For the CFU-E cell the phosphorylation rate of STAT, its export rate, the import rate of phosphorylated STAT and the time delay for the processes in the nucleus ($r_{\text{act}}, r_{\text{exp}}, r_{\text{imp2}}$ and r_{delay}) are unknown, and for the model of a NIH3T3 cell three of the parameters, $r_{\text{act}}, r_{\text{imp2}}$ and r_{delay}, are unknown. In Table 1, we summarize the parameter values used in our simulations.

The following theorem establishes the well-posedness of the above ODE system, particularly that its solution is uniformly bounded and for non-negative data also non-negative. The proof employs a standard result from Numerical Linear Algebra, which is stated in Lemma 3.2, below. This analysis is intended as preparation for corresponding results in the context of the more realistic mixed PDE-ODE models, which are the main theme of this paper.

Theorem 3.1. *For the given set of data the system (3.1) - (3.5) is well-posed. There is a unique global solution* $u = (u_0, \ldots, u_7)$, *with* $u_i \in C^1[0,\infty)$. *This solution is smooth, non-negative, uniformly bounded, and Lyapunov stable. For* $t \to \infty$, *it converges to a limit state* u^∞.

Proof. (i) *Rescaling:* We introduce the new scaled variables

$$v_i := v_{\text{cyt}} u_i, \;\; i = 0, 1, \quad v_i := v_{\text{nuc}} u_i, \;\; i = 2, \ldots, 7.$$

Using this notation the ODE system (3.1) - (3.5) can be rewritten in the form

$$v_0'(t) = -\frac{r_{\text{act}}\text{pJAK}(t)}{\nu_{\text{cyt}}} v_0(t) - \frac{r_{\text{imp}}}{\nu_{\text{cyt}}} v_0(t) + \frac{r_{\text{exp}}}{\nu_{\text{nuc}}} v_2(t), \tag{3.10}$$

$$v_1'(t) = -\frac{r_{\text{imp2}}}{\nu_{\text{cyt}}} v_1(t) + \frac{r_{\text{act}}\text{pJAK}(t)}{\nu_{\text{cyt}}} v_0(t), \tag{3.11}$$

$$v_2'(t) = -\frac{r_{\text{exp}}}{\nu_{\text{nuc}}} v_2(t) + \frac{r_{\text{imp}}}{\nu_{\text{cyt}}} v_0(t) + \frac{r_{\text{delay}}}{\nu_{\text{nuc}}} v_7(t), \tag{3.12}$$

$$v_3'(t) = -\frac{r_{\text{delay}}}{\nu_{\text{nuc}}} v_3(t) + \frac{r_{\text{imp2}}}{\nu_{\text{cyt}}} v_1(t), \tag{3.13}$$

$$v_i'(t) = -\frac{r_{\text{delay}}}{\nu_{\text{nuc}}} v_i(t) + \frac{r_{\text{delay}}}{\nu_{\text{nuc}}} v_{i-1}(t), \quad i = 4,5,6,7. \tag{3.14}$$

This is a homogenous linear system for the new state vector $v = (v_0, .., v_7)$, which can be formulated in an abstract form as follows:

$$v'(t) + \text{A}(t)v(t) = 0, \ t \geq 0, \quad v(0) = v^0, \tag{3.15}$$

with the system matrix

$$\text{A}(t) = \begin{bmatrix} \frac{r_{\text{act}}\text{pJAK}(t)+r_{\text{imp}}}{\nu_{\text{cyt}}} & 0 & -\frac{r_{\text{exp}}}{\nu_{\text{nuc}}} & 0 & 0 & 0 & 0 & 0 \\ -\frac{r_{\text{act}}\text{pJAK}(t)}{\nu_{\text{cyt}}} & \frac{r_{\text{imp2}}}{\nu_{\text{cyt}}} & 0 & 0 & 0 & 0 & 0 & 0 \\ -\frac{r_{\text{imp}}}{\nu_{\text{cyt}}} & 0 & \frac{r_{\text{exp}}}{\nu_{\text{nuc}}} & 0 & 0 & 0 & 0 & -\frac{r_{\text{delay}}}{\nu_{\text{nuc}}} \\ 0 & -\frac{r_{\text{imp2}}}{\nu_{\text{cyt}}} & 0 & \frac{r_{\text{delay}}}{\nu_{\text{nuc}}} & 0 & 0 & 0 & 0 \\ 0 & 0 & 0 & -\frac{r_{\text{delay}}}{\nu_{\text{nuc}}} & \frac{r_{\text{delay}}}{\nu_{\text{nuc}}} & 0 & 0 & 0 \\ 0 & 0 & 0 & 0 & -\frac{r_{\text{delay}}}{\nu_{\text{nuc}}} & \frac{r_{\text{delay}}}{\nu_{\text{nuc}}} & 0 & 0 \\ 0 & 0 & 0 & 0 & 0 & -\frac{r_{\text{delay}}}{\nu_{\text{nuc}}} & \frac{r_{\text{delay}}}{\nu_{\text{nuc}}} & 0 \\ 0 & 0 & 0 & 0 & 0 & 0 & -\frac{r_{\text{delay}}}{\nu_{\text{nuc}}} & \frac{r_{\text{delay}}}{\nu_{\text{nuc}}} \end{bmatrix}.$$

We discuss some special properties of the matrix $\text{A}(t) = (a_{ij}(t))_{i,j=1}^{7}$. It has a diagonally dominant transpose $\text{A}(t)^T$, i. e., there holds

$$\sum_{j=1, j\neq i}^{7} |a_{ij}(t)| \leq |a_{ii}(t)|, \quad i = 1, \ldots, 7. \tag{3.16}$$

Since all diagonal elements $a_{ii}(t)$ are real positive, this implies that all Gerschgorin circles of $\text{A}(t)^T$ lie in the right complex halfplane. Obviously, $\lambda_0(t) = 0$ is a simple eigenvalue with eigenvector

$$w^{(0)}(t) = \Big(\frac{\nu_{\text{cyt}}}{\nu_{\text{nuc}}} \frac{r_{\text{delay}}}{r_{\text{act}}\text{pJAK(t)}} c, \frac{\nu_{\text{cyt}}}{\nu_{\text{nuc}}} \frac{r_{\text{delay}}}{r_{\text{imp2}}} c, \frac{r_{\text{delay}}(r_{\text{act}}\text{pJAK(t)} + r_{\text{imp}})}{r_{\text{exp}} r_{\text{act}}\text{pJAK(t)}} c, c, \ldots, c\Big),$$

for any $c \in \mathrm{R}$, which is obtained as solution of the homogeneous system

$$\begin{aligned}
v_{\mathrm{nuc}}(r_{\mathrm{act}}\mathrm{pJAK}(t) + r_{\mathrm{imp}})w_0^{(0)}(t) - v_{\mathrm{cyt}}r_{\mathrm{exp}}w_2^{(0)}(t) &= 0,\\
-r_{\mathrm{act}}\mathrm{pJAK}(t)\cdot w_0^{(0)}(t) + r_{\mathrm{imp2}}w_1^{(0)}(t) &= 0,\\
-v_{\mathrm{cyt}}r_{\mathrm{delay}}w_7^{(0)}(t) + v_{\mathrm{cyt}}r_{\mathrm{exp}}w_2^{(0)}(t) - v_{\mathrm{nuc}}r_{\mathrm{imp}}w_0^{(0)}(t) &= 0,\\
-v_{\mathrm{nuc}}r_{\mathrm{imp2}}w_1^{(0)}(t) + v_{\mathrm{cyt}}r_{\mathrm{delay}}w_3^{(0)}(t) &= 0,\\
-r_{\mathrm{delay}}w_i^{(0)}(t) + r_{\mathrm{delay}}w_{i+1}^{(0)}(t)) = 0, \quad i &= 3,4,5,6.
\end{aligned}$$

This reflects the conservation property (3.6). All other eigenvalues $\{\lambda_j(t), j = 1\ldots,7\}$ have positive real part and are likewise simple. Corresponding eigenvectors can be explicitly determined. The details of this tedious calculation are omitted. In particular, there are no purely imaginary eigenvalues, i. e., for the coefficients given the solution cannot develop time-periodic behavior.

Since the 8×8-matrix $A(t)$ has 8 simple eigenvalues it is diagonalizable and possesses a basis $\{w^{(0)}(t),\ldots,w^{(7)}(t)\}$ of (normalized) eigenvectors. The corresponding regular 8×8-matrix $\mathrm{W}(t) := [w^{(0)}(t),\ldots,w^{(7)}(t)]$ then transforms $\mathrm{A}(t)$ into diagonal form,

$$\mathrm{W}^{-1}(t)\mathrm{A}(t)\mathrm{W}(t) = \Lambda(t) := \mathrm{diag}(\lambda_i(t))_{i=0}^7. \tag{3.17}$$

For our choice of coefficients in the matrix $\mathrm{A}(t)$ the eigenvalues $\lambda_i(t)$ as well as the corresponding eigenvectors $w^{(i)}(t)$ can be assumed to be continuously differentiable functions with respect to time, which become constant for $t \geq T$, i. e., $a_{ij}(t) = a_{ij}$, $\Lambda(t) = \Lambda$, and $\mathrm{W}^{-1}(t) = \mathrm{W}^{-1}$, for $t \geq T$.

(ii) *Existence and uniqueness:* Since the system (3.15) is linear in v and continuous in t the existence of a unique global solution follows by standard results on ODE systems (theorem of Picard-Lindelöf and extension theorem). Further, on each finite time interval the solution depends Lipschitz continuously on the initial data $u(0)$.

(iii) *Non-negativity:* We note that the matrix $\mathrm{A}(t)$ is of "non-negative type", i. e., there holds

$$a_{ii}(t) > 0, \quad a_{ij}(t) \leq 0, \quad i,j = 1,\ldots,7,\ i \neq j. \tag{3.18}$$

This together with the diagonal dominance (3.16) of $\mathrm{A}(t)^T$ implies by Lemma 3.2, below, that for $k > 0$ the matrix $\mathrm{I} + k\mathrm{A}(t)$ is invertible with an elementwise positive inverse, $(\mathrm{I} + k\mathrm{A}(t))^{-1} > 0$. Now, we discretize the system (3.15) by the backward Euler scheme, which results in the sequence of stationary equations

$$(\mathrm{I} + k\mathrm{A}(t_m))V_k^m = V_k^{m-1},\ m \geq 1, \quad V_k^0 = v(0), \tag{3.19}$$

on an equidistant time grid $\{t_m = mk, m = 0,1,2,\ldots\}$. For this approximation, we have on any fixed time interval the following error estimate (see Hairer et al. [13]):

$$\max_{0\leq t_m\leq t} \|V_k^m - v(t_m)\| \leq c(t)k \max_{[0,t]} \|v''\|. \tag{3.20}$$

If only $v \in C^1[0,\infty)^8$, we still have $\max_{0\leq t_m\leq t}\|V_k^m - v(t_m)\| \to 0\ (k \to 0)$. Then, for our initial value, $v(0) \geq 0$, the monotonicity property $(\mathrm{I} + k\mathrm{A}(t))^{-1} > 0$ implies that all $V_k^m \geq 0$, $m \geq 0$.

Hence, considering the limit $k \to 0$ in the error estimate (3.20), we conclude that $v \geq 0$ for all time.

(iv) *Uniform boundedness and asymptotic convergence:* The conservation of the quantity (3.6) in time together with the non-negativity of the variables $v_0, \ldots, v_7$ immediately implies the uniform boundedness of this solution. In the next step, we prove its asymptotic convergence to some limit state, which as a by-product also yields an alternative proof of its boundedness without referring to the result of Lemma 3.2. Using the relation (3.17) the initial value problem (3.15) can be rewritten in the form

$$\mathrm{W}^{-1}(t)v'(t) + \Lambda(t)\mathrm{W}^{-1}(t)v(t) = 0, \;\; t \geq 0, \quad v(0) = v^0,$$

or with the new variable $y(t) := \mathrm{W}^{-1}(t)v(t)$,

$$y'(t) + \Lambda y(t) = (\mathrm{W}^{-1})'(t)v(t) + (\Lambda - \Lambda(t))y(t), \;\; t \geq 0, \quad y(0) = \mathrm{W}^{-1}(0)v^0.$$

From this, we conclude that

$$\frac{d}{dt}(e^{\lambda_i t} y_i(t)) = e^{\lambda_i t}((\mathrm{W}^{-1})'(t)v(t) + (\Lambda - \Lambda(t))y(t))_i,$$

for $i = 0, \ldots, 7$, and integrating over time,

$$y_i(t) = e^{-\lambda_i t}\Big\{y_i(0) + \int_0^t e^{\lambda_i s}((\mathrm{W}^{-1})'(s)v(s) + (\Lambda - \Lambda(s))y(s))_i \, ds\Big\}.$$

This implies that

$$\begin{aligned}\lim_{t\to\infty} y_0(t) = \lim_{t\to\infty} \Big\{(\mathrm{W}^{-1}(0)v^0)_0 + \int_0^T ((\mathrm{W}^{-1})'(s)v(s) \\ + (\Lambda - \Lambda(s))\mathrm{W}^{-1}(s)v(s))_0 \, ds\Big\} =: y_0^\infty,\end{aligned}$$

and, for $i = 1, \ldots, 7$,

$$\begin{aligned}\lim_{t\to\infty} y_i(t) = \lim_{t\to\infty} \Big\{e^{-\lambda_i t}\Big\{(\mathrm{W}^{-1}(0)v^0)_i + \int_0^T e^{\lambda_i s}((\mathrm{W}^{-1})'(s)v(s) \\ + (\Lambda - \Lambda(s))\mathrm{W}^{-1}(s)v(s))_i \, ds\Big\}\Big\} = 0.\end{aligned}$$

From these asymptotic relations, we infer that

$$\lim_{t\to\infty} v(t) = \lim_{t\to\infty} W(t)y(t) = Wy^\infty, \tag{3.21}$$

where $y^\infty := (y_0^\infty, 0 \ldots, 0)$.

(v) *Stability:* Since the initial value problem (3.15) is linear, the local L-continuity of its solution with respect to the initial value guaranteed by the theorem of Picard-Lindelöf together with the asymptotic convergence result (3.21) imply that the solution is also Lyapunov stable, i. e., for given $\varepsilon > 0$ there exists a $\delta(\varepsilon) > 0$ such that for any initial value z^*, satisfying $\|z^*\| < \delta(\varepsilon)$, the corresponding solution of the inital value problem

$$z'(t) + \mathrm{A}(t)z(t) = 0, \;\; t \geq t_*, \quad z(0) = z^*,$$

satisfies

$$\sup_{t\geq t_*} \|z(t)\| < \varepsilon.$$

This completes the proof of the theorem. □

Lemma 3.2. *Let* $\mathrm{A} \in \mathrm{R}^{d\times d}$ *be a real matrix with the usual additive decomposition* $\mathrm{A} = \mathrm{L} + \mathrm{D} + \mathrm{R}$ *in its lower, main and upper diagonal parts* L, D *and* R, *respectively. Suppose that A is of so-called "non-negative type", i. e.,* D *is regular and there holds elementwise* $\mathrm{D} \geq 0$ *and* $\mathrm{L} + \mathrm{R} \leq 0$. *Further, let* A *or its transpose* A^T *be "(weakly) diagonally dominant",*

$$\max_{i=1,\ldots,d} \Big\{ \frac{1}{|a_{ii}|} \sum_{j=1,\, j\neq i}^{d} |a_{ij}| \Big\} \leq 1, \quad \textit{or} \quad \max_{j=1,\ldots,d} \Big\{ \frac{1}{|a_{jj}|} \sum_{i=1, i\neq j}^{d} |a_{ij}| \Big\} \leq 1. \tag{3.22}$$

Then, for $k > 0$ *the matrix* $\mathrm{I} + k\mathrm{A}$ *is a so-called M-matrix, i. e., it is invertible with elementwise positive inverse,* $(\mathrm{I} + k\mathrm{A})^{-1} > 0$.

Proof. Though this result is well-known in Numerical Linear Algebra (see, e. g., Varga [25] or Bermon & Plemmons [4]), for the sake of completeness, we provide the short proof. Suppose that the matrix A is diagonally dominant. Then, the matrix $\mathrm{I} + k\mathrm{A}$ is also of non-negative type and even *strictly* diagonally dominant, i. e., the corresponding inequalities (3.22) hold with strict inequality signs. Hence by the theorem of Gerschgorin it follows that the corresponding so-called Jacobi matrix $\mathrm{J} := -k(\mathrm{I} + k\mathrm{D})^{-1}(\mathrm{L} + \mathrm{R}) \geq 0$ has spectral radius $\varrho(\mathrm{J}) < 1$. This implies that the matrix $\mathrm{I} - \mathrm{J}$ is regular with inverse

$$(\mathrm{I} - \mathrm{J})^{-1} = \sum_{k=0}^{\infty} \mathrm{J}^k = \mathrm{I} + \sum_{k=1}^{\infty} \mathrm{J}^k > 0.$$

From this, we infer the regularity of $\mathrm{I} + k\mathrm{A} = \mathrm{I} + k\mathrm{D} + k(\mathrm{L} + \mathrm{R}) = (\mathrm{I} + k\mathrm{D})(\mathrm{I} - \mathrm{J})$ and $(\mathrm{I} + k\mathrm{A})^{-1} = (\mathrm{I} - \mathrm{J})^{-1}(\mathrm{I} + k\mathrm{D})^{-1} > 0$. If A^T is assumed to be diagonally dominant the argument is analogous. □

Remark 3.3. As a by-product of the proof of Theorem 3.1, we see that the first-order backward Euler scheme applied to the system (3.1) - (3.5) yields non-negative approximations $U^m \geq 0$ at all discrete time levels $t_m \geq 0$, which satisfy the error estimate

$$\max_{0\leq t_m \leq T} \|U^m - u(t_m)\| \leq c(T) k \max_{t\in[0,T]} \|u''(t)\|. \tag{3.23}$$

In general the error constant $c(T)$ grows exponentially in T due to the use of Gronwall's inequality in the proof. In the present special situation of a diagonally dominant and diagonalizable system matrix $\mathrm{A}(t)$ this growth can be shown to be only linear, which, however, will not be further pursued here. Analogous results do not necessarily hold true for higher-order time-stepping schemes, such as for example the backward differencing formulas BDF(R) ($R \geq 2$). In the computations described in Section 4, below, we have therefore used the simple backward Euler method though it is only of first order.

3.2 A PDE-ODE Model

To address the biological question described above, we add diffusion for unphosphorylated and phosphorylated STAT in the cytoplasm in our model. Different transport processes can be modeled by different diffusion coefficients. At first, we model free diffusion using a constant diffusion coefficient based on measurements by fluorescence correlation spectroscopy. The diffusion coefficient $D = 15\ \mu m^2/s$ was used in the simulations. The additional transport of the molecules along the microtubules is modeled for the NIH3T3 cell through an anisotropic diffusion coefficient whereas the mainstream direction of STAT movement was set in the y-direction of the cell. Our goal here was not to compare two diffusion processes where the trace of the diffusion coefficient must be equal. We introduced additional transport on the microtubule by inserting a faster diffusion coefficient in the direction towards the nucleus (y-direction). Of coarse, the more realistic description would be to add a transport term to the equations.

To answer the biological question posed only the cytoplasm Ω_{cyt} has to be dissolved spatially. The processes in the nucleus such as DNA binding and dephosphorylation of STAT do not have to be known in detail. For their description it is sufficient to use time delays as black box elements. As already described in the previous section, phosphorylation as well as nuclear import and export of STAT only occurs at the boundaries of the cytoplasm. For this specific question, we therefore obtain a mixed system of linear differential equations: two diffusion equations with linear Robin boundary conditions and six ODEs, two of them are coupled to the PDEs through the import terms and the other four describe the processes in the nucleus by linear delay equations:

i) Cytoplasm Ω_{cyt}, for $(t,x) \in (0,\infty)\times\Omega_{cyt}$:

$$\partial_t u_0(t,x) = D\Delta u_0(t,x), \tag{3.24}$$

$$\partial_t u_1(t,x) = D\Delta u_1(t,x). \tag{3.25}$$

ii) Nucleus Ω_{nuc}, for $t \in (0,\infty)$:

$$v_{nuc}u_2'(t) = -r_{exp}u_2(t) + r_{delay}u_7(t) + \frac{r_{imp}}{|\partial\Omega_{nuc}|}\int\limits_{\partial\Omega_{nuc}} u_0(t,x)\,do_x, \tag{3.26}$$

$$v_{nuc}u_3'(t) = -r_{delay}u_3(t) + \frac{r_{imp2}}{|\partial\Omega_{nuc}|}\int\limits_{\partial\Omega_{nuc}} u_1(t,x)\,do_x, \tag{3.27}$$

$$v_{nuc}u_i'(t) = -r_{delay}u_i(t) + r_{delay}u_{i-1}(t), \quad i = 4,5,6,7. \tag{3.28}$$

The initial conditions are essentially the same as used in the previous section for the pure ODE model, (3.29)-(3.31):

$$u_1(0,x) = 0,\ \ x \in \Omega_{cyt}, \quad u_3(0) = u_4(0) = u_5(0) = u_6(0) = u_7(0) = 0, \tag{3.29}$$

$$\text{CFU-E:} \quad u_0(0,x) = 50\ \text{mol}/\mu m^3,\ \ x \in \Omega, \quad u_2(0) = 18\ \text{mol}/\mu m^3, \tag{3.30}$$

$$\text{NIH3T3:} \quad u_0(0,x) = 16\ \text{mol}/\mu m^3, x \in \Omega, \quad u_2(0) = 20\ \text{mol}/\mu m^3. \tag{3.31}$$

We only have to observe that the concentrations of unphosphorylated and phosphorylated STAT molecules in the cytoplasm, $u_0(t,x)$ and $u_1(t,x)$, are now space dependent. The

phosphorylation as well as the import and export of molecules enter through the linear Robin boundary conditions:

$$D\partial_n u_0(t,x) = -\frac{r_{\text{act}}}{|\partial\Omega_{\text{cyt}}|}\text{pJAK}(t,x)u_0(t,x), \quad \text{on } \partial\Omega_{\text{cyt}}, \tag{3.32}$$

$$D\partial_n u_0(t,x) = -\frac{r_{\text{imp}}}{|\partial\Omega_{\text{cyt}}|}u_0(t,x) + \frac{r_{\text{exp}}}{|\partial\Omega_{\text{nuc}}|}u_2(t), \quad \text{on } \partial\Omega_{\text{nuc}}, \tag{3.33}$$

$$D\partial_n u_1(t,x) = \frac{r_{\text{act}}}{|\partial\Omega_{\text{cyt}}|}\text{pJAK}(t,x)u_0(t,x), \quad \text{on } \partial\Omega_{\text{cyt}}, \tag{3.34}$$

$$D\partial_n u_1(t,x) = -\frac{r_{\text{imp2}}}{|\partial\Omega_{\text{nuc}}|}u_1(t,x), \quad \text{on } \partial\Omega_{\text{nuc}}, \tag{3.35}$$

where $\partial\Omega_{\text{cyt}}$ denotes the outer boundary of the cell, i.e. the membrane, and $\partial\Omega_{\text{nuc}}$ the boundary of the nucleus. A problem with prescribing these spatially constant Robin-boundary-conditions is that this may introduce incompatibilities with the initial conditions along the boundary preventing the solution from being smooth down to $t = 0$. In fact, there holds:

$$\begin{aligned}
D\partial_n u_0(0,x) &= -\frac{r_{\text{act}}}{|\partial\Omega_{\text{cyt}}|}\text{pJAK}(0,x)u_0(0,x) = 0, \quad x \in \partial\Omega_{\text{cyt}},\\
D\partial_n u_0(0,x) &= -\frac{r_{\text{imp}}}{|\partial\Omega_{\text{nuc}}|}u_0(0,x) + \frac{r_{\text{exp}}}{|\partial\Omega_{\text{nuc}}|}u_2(0) = C \approx 243, \quad x \in \partial\Omega_{\text{nuc}},\\
D\partial_n u_1(0,x) &= \frac{r_{\text{act}}}{|\partial\Omega_{\text{cyt}}|}\text{pJAK}(0,x)u_0(t,x) = 0, \quad x \in \partial\Omega_{\text{cyt}},\\
D\partial_n u_1(0,x) &= -\frac{r_{\text{imp2}}}{|\partial\Omega_{\text{nuc}}|}u_1(0,x) = 0, \quad x \in \partial\Omega_{\text{nuc},}.
\end{aligned}$$

On the boundary $\partial\Omega_{\text{cyt}}$ the Robin boundary conditions are compatible with our initial conditions, only the boundary condition for u_0 on $\partial\Omega_{\text{nuc}}$ does not fit the proposed simplified initial condition which, however, is also not fully biologically correct. The non-activated molecules shuttle permanently between the cytoplasm and the nucleus with different import and export parameters which are cell-type dependent. Thus, the concentration of the molecules cannot stay constant up to the boundary $\partial\Omega_{\text{nuc}}$. We will introduce a little change in the initial condition to guarantee the smoothness of u_0 down to time $t = 0$. This is accomplished by introducing a smooth function $\chi(x)$, which fits the constant initial value in the interior domain to the value which fulfills the Robin boundary conditions $u_0(0,s) = \frac{r_{\text{exp}}}{r_{\text{imp}}}u_2(0)$ on $\partial\Omega_{\text{nuc}}$. For the CFU-E cell there holds $u_0(0,s) \approx 6.8\,u_2(0) = 122$, so $\chi(x)$ has to fit smoothly the endvalues 50 to 122, whereas for the NIH3T3 cell there holds $u_0(0,s) \approx 0.7\,u_2(0) = 14$, so the values 16 and 14 have to be connected smoothly. The modified initial condition is then $\tilde{u}_0(0,x) = \chi(x)u(0,x)$. On $\partial\Omega_{\text{cyt}}$ the presence of the smooth parameter function pJAK(t,x) guarantees the smoothness of the solution down to time $t = 0$.

Using the space-independent averaged unknowns

$$\bar{u}_0(t) := \frac{1}{|\Omega_{\text{cyt}}|}\int_{\Omega_{\text{cyt}}} u_0(t,x)\,dx, \quad \bar{u}_1(t) := \frac{1}{|\Omega_{\text{cyt}}|}\int_{\Omega_{\text{cyt}}} u_1(t,x)\,dx,$$

we reformulate equations (3.24) and (3.25) as

$$\begin{aligned}
\frac{|\Omega_{\text{cyt}}|}{D}\overline{u}_0'(t) &= \int_{\Omega_{\text{cyt}}} \Delta u_0(t,x)\,dx = \int_{\partial\Omega_{\text{cyt}}\cup\partial\Omega_{\text{nuc}}} \partial_n u_0(t,x)\,do_x \\
&= -\frac{r_{\text{act}}}{|\partial\Omega_{\text{cyt}}|}\int_{\partial\Omega_{\text{cyt}}\cup\partial\Omega_{\text{nuc}}} \text{pJAK}(t,x)u_0(t,x)\,do_x \\
&\quad -\frac{r_{\text{imp}}}{|\partial\Omega_{\text{nuc}}|}\int_{\partial\Omega_{\text{nuc}}} u_0(t,x)\,do_x + \frac{r_{\text{exp}}}{|\partial\Omega_{\text{nuc}}|}u_2(t), \\
\frac{|\Omega_{\text{cyt}}|}{D}\overline{u}_1'(t) &= \int_{\Omega_{\text{cyt}}} \Delta u_1(t,x)\,dx = \int_{\partial\Omega_{\text{cyt}}\cup\Omega_{\text{nuc}}} \partial_n u_1(t,x)\,do_x \\
&= \frac{r_{\text{act}}}{|\partial\Omega_{\text{cyt}}|}\int_{\partial\Omega_{\text{cyt}}} \text{pJAK}(t,x)u_0(t,x)\,do_x - \frac{r_{\text{imp2}}}{|\partial\Omega_{\text{nuc}}|}\int_{\partial\Omega_{\text{nuc}}} u_1(t,x)\,do_x.
\end{aligned}$$

Adding these two equations with (3.26) - (3.28), we see that now the quantity

$$\sigma := D^{-1}|\Omega_{\text{cyt}}|(\overline{u}_0+\overline{u}_1) + |\Omega_{\text{nuc}}|(u_2+u_3+u_4+u_5+u_6+u_7)$$

is conserved in time as required for physical reasons. For the state vector $\overline{u} := (\overline{u}_0, \overline{u}_1, u_2, \dots, u_7)$, we have the following system of ODEs:

$$\begin{aligned}
\frac{|\Omega_{\text{cyt}}|}{D}\overline{u}_0'(t) &= -\frac{r_{\text{act}}}{|\partial\Omega_{\text{cyt}}|}\int_{\partial\Omega_{\text{cyt}}} \text{pJAK}(t,x)u_0(t,x)\,do_x \\
&\quad + \frac{r_{\text{imp}}}{|\partial\Omega_{\text{nuc}}|}\int_{\partial\Omega_{\text{nuc}}} u_0(t,x)\,do_x + \frac{r_{\text{exp}}}{|\partial\Omega_{\text{nuc}}|}u_2(t),
\end{aligned} \tag{3.36}$$

$$\begin{aligned}
\frac{|\Omega_{\text{cyt}}|}{D}\overline{u}_1'(t) &= \frac{r_{\text{act}}}{|\partial\Omega_{\text{cyt}}|}\int_{\partial\Omega_{\text{cyt}}} \text{pJAK}(t,x)u_0(t,x)\,do_x \\
&\quad - \frac{r_{\text{imp2}}}{|\partial\Omega_{\text{nuc}}|}\int_{\partial\Omega_{\text{nuc}}} u_1(t,x)\,do_x,
\end{aligned} \tag{3.37}$$

$$|\Omega_{\text{nuc}}|u_2'(t) = -r_{\text{exp}}u_2(t) + r_{\text{delay}}u_7(t) + \frac{r_{\text{imp}}}{|\partial\Omega_{\text{nuc}}|}\int_{\partial\Omega_{\text{nuc}}} u_0(t,x)\,do_x, \tag{3.38}$$

$$|\Omega_{\text{nuc}}|u_3'(t) = -r_{\text{delay}}u_3(t) + \frac{r_{\text{imp2}}}{|\partial\Omega_{\text{nuc}}|}\int_{\partial\Omega_{\text{nuc}}} u_1(t,x)\,do_x, \tag{3.39}$$

$$|\Omega_{\text{nuc}}|u_i'(t) = -r_{\text{delay}}u_i(t) + r_{\text{delay}}u_{i-1}(t), \quad i = 4,5,6,7. \tag{3.40}$$

The following theorem contains the main results of this paper. For its formulation, we use the standard notation of space-time function spaces. For a real function Banach space X, with norm $\|\cdot\|$ on a bounded domain $\Omega \subset \mathbb{R}^n$, the space $L^p(0,T;X)$ consists of all measurable functions $u : [0,T] \to X$ with

$$\|u\|_{L^p(0,T;X)} := \Big(\int_0^T \|u(t)\|^p\,dt\Big)^{1/p} < \infty, \tag{3.41}$$

for $1 \le p < \infty$, and $\|u\|_{L^\infty(0,T;X)} := \operatorname{ess\,sup}_{(0,T)}\|u(t)\| < \infty$. In the present case, we take $V := H^1(\Omega)$ with dual space $V^* = H^{-1}(\Omega)$ and $H := L^2(\Omega)$ and consider the usual Gelfand

triple $V \hookrightarrow H \hookrightarrow V^*$. We denote by $(\cdot,\cdot)_\Omega$ and $(\cdot,\cdot)_\Gamma$ the usual L^2 scalar products over the domain Ω and a part $\Gamma \subset \partial\Omega$ of its boundary, respectively, and by $\|\cdot\|_\Omega$ and $\|\cdot\|_\Gamma$ the corresponding norms.

Theorem 3.4. *For the given set of data the initial-boundary value problem (3.24) - (3.35) is well-posed. There is a unique global solution $u = (u_1,\dots,u_7)$, with $u_0, u_1 \in L^2(0,T;V)$, $\partial_t u_0, \partial_t u_1 \in L^2(0,T;V^*)$, and $u_2,\dots,u_7 \in C^1[0,T]$ on any time interval $[0,T]$. Further, for sufficiently smooth and compatible data this solution is likewise smooth, non-negative, uniformly bounded and Lyapunov stable.*

The proof of this theorem will be given in the following two sections. Though the problem (3.24) - (3.28) is linear, we use an "energy technique" and a fixed-point argument based on its variational formulation rather than the common spectral or semigroup approach in order to prepare for more general non-autonomous and nonlinear versions of the model such as described in Remark 3.5.

Remark 3.5. We note that the coefficients pJAK(t,x) in the Robin boundary condition explicitly depends on time making the coupled system (3.24) - (3.28) non-autonomous. Furthermore, our simplified model involves already dimerized molecules with concentrations u_i, $i = 0,\dots 3$. By considering every monomer and every reaction taking place in the cytoplasm, the resulting system would contain nonlinear terms such as u_i^2 for dimers, u_i^3, $u_i^2 u_j$, and $u_i u_j u_k$ for trimers and so on for multicomplexes. For these additional equations must be considered (see [8]),

$$\partial_t u_0(t,x) = D\Delta u_0(t,x), \tag{3.42}$$

$$\partial_t u_1(t,x) = D\Delta u_1(t,x) - 2k_1 u_1^2 u_3 + 2k_2 u_2, \tag{3.43}$$

$$\partial_t u_2(t,x) = D\Delta u_2(t,x) + k_1 u_1^2 u_3 - k_2 u_2, \tag{3.44}$$

$$\partial_t u_3(t,x) = D\Delta u_3(t,x) - k_1 u_1^2 u_3 + k_2 u_2. \tag{3.45}$$

As mentioned before, due to the possibility of measuring the activated JAK molecules for this model, we do not need to consider the detailed receptor model. Otherwise, additional non-linear terms would appear in the Robin boundary conditions (3.32) and (3.34) of the form

$$D\partial_n u_0(t,\partial\Omega_{\rm cyt}) = -\gamma \frac{k_a R u_0^n}{k_M + u_0^n},$$

which describes the cooperativity of binding to the receptor. For $0 < n < 1$ the reaction is negatively cooperative, for $n = 1$ non-cooperative and for $n > 1$ positively cooperative. The general argument used below for proving the well-posedness of the *linear* coupled system (3.24) - (3.28) is expected to be extendable to certain *nonlinear* models of this type. This will be the subject of a forthcoming paper.

3.3 Proof of global existence and uniqueness

The mixed system (3.24) - (3.35) of reaction-diffusion equations and ordinary differential equations is coupled through the concentration $u_2(t)$ of the non-activated STAT in the

boundary condition (3.33) on the nucleus boundary $\partial\Omega_{\text{nuc}}$. This motivates the iterative decoupling of the two system parts and the use of the Banach fixed-point theorem for proving the existence of a solution to the coupled system [18].

(i) *Fixed-point mapping:* On some finite time interval $[t_0, t_1] \subset [0, \infty)$ and for a certain given $a \in \mathbb{R}_+$, we define

$$C_a[t_0, t_1] := \{v \in C[t_0, t_1] \mid v(t_0) = a\}.$$

On this manifold, we consider the mapping $\chi : C_a[t_0, t_1] \to C_a[t_0, t_1]$, acting on the coupling variable u_2, which for some given $\hat{u}_2 \in C_a[t_0, t_1]$ is defined by $u_2 = \chi(\hat{u}_2)$ where $u = (u_0, \ldots, u_7)$ is the solution of the following coupled PDE-ODE system:

Cytoplasm Ω_{cyt}, for $(t, x) \in (t_0, t_1] \times \Omega_{\text{cyt}}$:

$$\partial_t u_0(t, x) = D\Delta u_0(t, x), \tag{3.46}$$

$$\partial_t u_1(t, x) = D\Delta u_1(t, x). \tag{3.47}$$

Nucleus Ω_{nuc}, for $t \in (t_0, t_1]$:

$$(u_2)'(t) + \frac{r_{\text{exp}}}{|\Omega_{\text{nuc}}|} u_2(t) = \frac{r_{\text{delay}}}{|\Omega_{\text{nuc}}|} u_7(t) + \frac{r_{\text{imp}}}{|\Omega_{\text{nuc}}||\partial\Omega_{\text{nuc}}|} \int\limits_{\partial\Omega_{\text{nuc}}} u_0(t, s)\, do_x, \tag{3.48}$$

$$(u_3)'(t) + \frac{r_{\text{delay}}}{|\Omega_{\text{nuc}}|} u_3(t) = \frac{r_{\text{imp2}}}{|\Omega_{\text{nuc}}|\partial\Omega_{\text{nuc}}|} \int\limits_{\partial\Omega_{\text{nuc}}} u_1(t, s)\, do_x, \tag{3.49}$$

$$(u_i)'(t) + \frac{r_{\text{delay}}}{|\Omega_{\text{nuc}}|} u_i(t) = \frac{r_{\text{delay}}}{|\Omega_{\text{nuc}}|} u_{i-1}(t), \quad i = 4, 5, 6, 7, \tag{3.50}$$

with the Robin boundary conditions

$$D\partial_n u_0(t, x) = -\frac{r_{\text{act}}}{|\partial\Omega_{\text{cyt}}|} \text{pJAK}(t) u_0(t, x), \quad \text{on } \partial\Omega_{\text{cyt}}, \tag{3.51}$$

$$D\partial_n u_0(t, x) = -\frac{r_{\text{imp}}}{|\partial\Omega_{\text{nuc}}|} u_0(t, x) + \frac{r_{\text{exp}}}{|\partial\Omega_{\text{nuc}}|} \hat{u}_2(t), \quad \text{on } \partial\Omega_{\text{nuc}}, \tag{3.52}$$

$$D\partial_n u_1(t, x) = \frac{r_{\text{act}}}{|\partial\Omega_{\text{cyt}}} \text{pJAK}(t) u_0(t, x), \quad \text{on } \partial\Omega_{\text{cyt}}, \tag{3.53}$$

$$D\partial_n u_1(t, x) = -\frac{r_{\text{imp2}}}{|\partial\Omega_{\text{nuc}}|} u_1(t, x), \quad \text{on } \partial\Omega_{\text{nuc}}, \tag{3.54}$$

and the initial values

$$u_0(t_0, x), u_1(t_0, x), \ x \in \Omega_{\text{cyt}}, \quad u_2(t_0), ..., u_7(t_0), \tag{3.55}$$

chosen according to (3.29) - (3.31).

For proving that the mapping $\chi : C_a[t_0, t_1] \to C_a[t_0, t_1]$ is well defined, we use standard methods from the literature. Existence results for parabolic problems with Dirichlet boundary conditions can be found in Ladyženskaja et al. [15], Jost [14], Wloka [26], Liebermann [16], for those with Neumann boundary conditions in [15], [14], and those for Robin boundary conditions also in [15] and [16]. In the following, we will use a generic constant $c \geq 0$, which may vary with the context.

Lemma 3.6. *Let D be a positive constant, $d \in C([0,T])$ a continuous non-negative function and $\Omega = \Omega_{cyt}$ with $\partial\Omega = \partial\Omega_{cyt} \cup \partial\Omega_{nuc}$. Then, for any initial value $v_0 \in H$ and boundary data $g(x,t) \in L^2(0,T;H^{-1/2}(\partial\Omega))$ the initial-value problem with Robin boundary conditions*

$$\begin{aligned} \partial_t v(t,x) &= D\Delta v(t,x), \quad (t,x) \in (0,T] \times \Omega, \\ D\partial_n v(t,x) + d(t)v(t,x) &= g(t,x), \quad (t,x) \in (0,T] \times \partial\Omega, \\ v(0,x) &= v^0, \quad x \in \Omega, \end{aligned} \tag{3.56}$$

has a unique solution $v \in W(0,T)$, where

$$W(0,T) := \{v \in L^2(0,T,V) \cap C([0,T],H) \,|\, \partial_t v \in L^2(0,T,V^*)\}.$$

Further there holds the a priori estimate

$$\|v\|_{L^\infty(0,T;H)} + \|v\|_{L^2(0,T;V)} \le c\|v^0\|_\Omega + c\|g\|_{L^\infty(0,T;H^{-1/2}(\partial\Omega))}. \tag{3.57}$$

Proof. We consider the usual variational formulation of the system (3.56) using test functions $\varphi \in V$ for $t \in [0,T]$:

$$(\partial_t v, \varphi) + D(\nabla v, \nabla\varphi) + d(t)(v,\varphi)_{\partial\Omega} = (g,\varphi)_{\partial\Omega}. \tag{3.58}$$

For the following, we introduce the abbreviations

$$a(t;\psi,\varphi) := D(\nabla\psi,\nabla\varphi) + d(t)(\psi,\varphi)_{\partial\Omega}, \qquad h(t;\varphi) := (g,\varphi)_{\partial\Omega}.$$

The boundedness of the bilinear form $a(t;\,\cdot\,,\,\cdot\,)$ can be shown by using a (suboptimal) trace inequality (see Adams & Fournier [1] or Wloka [26]),

$$\begin{aligned} |a(t;\psi,\varphi)| &= |D(\nabla\psi,\nabla\varphi) + d(t)(\psi,\varphi)_{\partial\Omega}| \\ &\le D\|\nabla\psi\|\|\nabla\varphi\| + d(t)\|\psi\|_{\partial\Omega}\|\varphi\|_{\partial\Omega} \\ &\le D\|\nabla\psi\|\|\nabla\varphi\| + d(t)\|\psi\|_V\|\varphi\|_V \\ &\le c\|\psi\|_V\|\varphi\|_V, \end{aligned} \tag{3.59}$$

and its coercitivity by applying the generalized Poincaré inequality,

$$a(t;\psi,\psi) = D\|\nabla\psi\|^2 + d(t)\|\psi\|^2_{\partial\Omega} \ge c\|\psi\|^2. \tag{3.60}$$

In virtue of (3.59) and (3.60), we obtain from the standard theory (see Wloka [26]) the existence of a unique solution $v \in W(0,T)$ of the parabolic problem

$$(\partial_t v,\varphi) + a(t;v,\varphi) = h(t;\varphi), \quad \forall\varphi \in V,\ t \in (0,T], \quad v|_{t=0} = v^0, \tag{3.61}$$

and the a priori estimate

$$\|u\|_{L^\infty(0,T;H)} + \|u\|_{L^2(0,T;V)} \le c\|v^0\|_\Omega + c\|g\|_{L^2(0,T;H^{-1/2}(\partial\Omega))}. \tag{3.62}$$

This concludes the proof of the lemma. □

In the considered PDE-ODE model the boundary of Ω consists of two disjoint parts, $\partial\Omega = \partial\Omega_{\text{nuc}} \cup \partial\Omega_{\text{cyt}}$. We have the trivial embedding $C_a[t_0,t_1] \subset L^2(t_0,t_1;H^{-1/2}(\partial\Omega)$ by interpreting constants as constant functions on Ω. Hence, for given $\hat{u}_2 \in C_a[t_0,t_1]$ on some time interval $[t_0,t_1]$, from Lemma 3.6, we obtain $u_0 \in W(t_0,t_1)$, which solves (3.46) together with (3.51) and (3.52). Further, there holds

$$\int_{\partial\Omega} u_0(\cdot,x)\,do_x \in C[t_0,t_1], \quad u_0|_{\partial\Omega_{\text{cyt}}} \in L^2(t_0,t_1;H^{-1/2}(\partial\Omega_{\text{cyt}})).$$

Then, again from Lemma 3.6, we also obtain $u_1 \in W(t_0,t_1)$ satisfying (3.47) together with (3.53) and (3.54) and also

$$\int_{\partial\Omega} u_1(\cdot,x)\,do_x \in C[t_0,t_1].$$

Thus, the right hand side of (3.49) is continuous in time implying the existence of a solution $u_3 \in C[t_0,t_1]$. Following the same arguments, we conclude the existence of $u_4,u_5,u_6,u_7 \in C[t_0,t_1]$ and consequently also of $u_2 \in C[t_0,t_1]$. Observing $u_2(t_0) = a$, we see that $\chi(u_2) \in C_a[t_0,t_1]$.

(ii) Contraction property: Next, we show that the mapping $\chi(\cdot) : C_a[t_0,t_1] \to C_a[t_0,t_1]$ is a contraction with respect to the natural norm $\|\cdot\|_\infty$ of $C[t_0,t_1]$. Let $\hat{u}_2,\hat{v}_2 \in C_a[t_0,t_1]$ be given and let u,v be the corresponding solutions constructed in (i), such that $u_2 = \chi(\hat{u}_2), v_2 = \chi(\hat{u}_2) \in C_a[t_0,t_1]$. We will derive a priori estimates for the difference $w := u_2 - v_2$, with initial value $w(t_0) = 0$, in terms of $\hat{w} := \hat{u}_2 - \hat{v}_2$. For simplicity, we set all the parameters in the equations (3.46) - (3.55) equal to one. The following argument works in the same way with the specific values because all parameters are constant and positive and pJAK(t) is a continuous, positive, and bounded function.

First, using the variational form of equations (3.46) and (3.47), we can bound the first two components w_0 and w_1 in terms of w_2. On the time interval $[t_0,t_1]$, we have

$$(\partial_t w_0,\varphi)_\Omega + (\nabla w_0,\nabla\varphi)_\Omega + (w_0,\varphi)_{\partial\Omega_{\text{nuc}}} + (w_0,\varphi)_{\partial\Omega_{\text{cyt}}} = (\hat{w}_2,\varphi)_{\partial\Omega_{\text{nuc}}}, \tag{3.63}$$

for $\varphi \in V$. We choose $\varphi = w_0$ and estimate the right hand side $(\hat{w}_2,w_0)_{\partial\Omega_{\text{nuc}}}$ using Hölder's and Young's inequality as follows:

$$(\hat{w}_2,w_0)_{\partial\Omega_{\text{nuc}}} \le \varepsilon\|w_0\|^2_{\partial\Omega_{\text{nuc}}} + c\varepsilon^{-1}\hat{w}_2^2, \quad \varepsilon > 0. \tag{3.64}$$

For ε sufficiently small the first term in the right hand side can be absorbed into the left hand side of (3.63) yielding

$$(\partial_t w_0,w_0)_\Omega + \|\nabla w_0\|^2_\Omega + \|w_0\|^2_{\partial\Omega_{\text{nuc}}} \le c\hat{w}_2^2. \tag{3.65}$$

Integrating this with respect to time and using the trace theorem, we conclude that

$$\int_{t_0}^{t_1} \|w_0\|^2_{\partial\Omega_{\text{cyt}}}\,dt + \int_{t_0}^{t_1} \|w_0\|^2_{\partial\Omega_{\text{nuc}}}\,dt \le c\int_{t_0}^{t_1} \hat{w}_2^2\,dt. \tag{3.66}$$

For the second component w_1, we proceed in the same way. Using the corresponding variational formulation with $\varphi = w_1$, we get

$$(\partial_t w_1,w_1)_\Omega + \|\nabla w_1\|^2_\Omega + \|w_1\|^2_{\partial\Omega_{\text{nuc}}} = (w_0,w_1)_{\partial\Omega_{\text{cyt}}}. \tag{3.67}$$

Again using Hölder's and Young's inequality, we estimate

$$(w_0, w_1)_{\partial\Omega_{\rm cyt}} \le \varepsilon \|w_1\|^2_{\partial\Omega_{\rm cyt}} + c\varepsilon^{-1}\|w_0\|^2_{\partial\Omega_{\rm cyt}}, \quad \varepsilon > 0. \tag{3.68}$$

We apply the trace theorem and the generalized Poincaré inequality to obtain

$$\|w_1\|_{\partial\Omega_{\rm cyt}} \le c\|w_1\|_V \le c(\|\nabla w_1\|_\Omega + \|w_1\|_{\partial\Omega_{\rm nuc}}). \tag{3.69}$$

With a suitable choice of ε, we can absorb the term from the right hand side in (3.69) into the left hand side of (3.67) and obtain after integration over time

$$\int_{t_0}^{t_1} \|w_1\|^2_{\partial\Omega_{\rm nuc}}\, dt \le c \int_{t_0}^{t_1} \hat{w}_2^2\, dt. \tag{3.70}$$

The solution components $w_3, \dots, w_7$ are not space dependent. From the equations (3.49) and (3.50), we obtain

$$\int_{t_0}^{t_1} w_3^2\, dt \le c \int_{t_0}^{t_1} \|w_1\|^2_{\partial\Omega_{\rm nuc}}\, dt \le c \int_{t_0}^{t_1} \hat{w}_2^2\, dt, \tag{3.71}$$

$$\int_{t_0}^{t_1} w_i^2\, dt \le c \int_{t_0}^{t_1} w_{i-1}^2\, dt \le c \int_{t_0}^{t_1} \hat{w}_2^2\, dt, \quad i = 4,5,6,7. \tag{3.72}$$

So far, we have bounded each of the functions w_i, $i = 0,1,3,\dots,7$, in terms of $\hat{w}_2$. Finally, from equation (3.48), we derive in the standard way

$$\begin{aligned} \int_{t_0}^{t_1} (w_2 w_2' + w_2^2)\, dt &= \int_{t_0}^{t_1} \Big(w_7 w_2 + w_2 \int_{\partial\Omega_{\rm nuc}} w_0\, ds \Big) dt \\ &\le \varepsilon \int_{t_0}^{t_1} w_2^2\, dt + \frac{c}{\varepsilon} \int_{t_0}^{t_1} \{ w_7^2 + \|w_0\|^2_{\partial\Omega_{\rm nuc}} \}\, dt. \end{aligned} \tag{3.73}$$

Hence, taking ε sufficiently small and using (3.66) and (3.72), we obtain

$$\tfrac{1}{2} w_2(t_1)^2 \le \int_{t_0}^{t_1} (\tfrac{1}{2}(w_2^2)' + w_2^2)\, dt \le c \int_{t_0}^{t_1} \hat{w}_2^2\, dt \le c|t_1 - t_0| \|\hat{w}_2\|^2_\infty. \tag{3.74}$$

Considering $t_1 > t_0$ as a free variable, we finally obtain on the time interval $[t_0, t_1]$ that

$$\|\chi(u_2) - \chi(v_2)\|^2_\infty = \|w_2\|^2_\infty \le c(t_1 - t_0)\|\hat{w}_2\|^2_\infty = c(t_1 - t_0)\|\hat{u}_2 - \hat{v}_2\|^2_\infty. \tag{3.75}$$

Hence, for a sufficiently small time interval $[t_0, t_1]$, we have $c(t_1 - t_0) < 1$ such that the fixed-point mapping $\chi(\cdot)$ becomes a contraction. The space $C[t_0, t_1]$ equipped with the maximum norm is a Banach space and the linear manifold $C_a[t_0, t_1]$ is a closed subset of $C[t_0, t_1]$. Hence, the Banach fixed-point theorem applies and yields the existence of a unique fixed point $u_2 \in C_a[t_0, t_1]$ of the mapping $\chi(\cdot)$. This then gives us a unique local solution $u = (u_i)_{i=0}^7$ on the time interval $[t_0, t_1]$ of the system (3.24) - (3.35).

For later purposes, we note that this fixed-point $u_2 \in C_a[t_0, t_1]$ is obtained as limit of the usual fixed-point iteration (successive iteration)

$$u_2^{k+1} = \chi(u_2^k), \quad k \in \mathbb{N}, \tag{3.76}$$

with starting value $u_2^0 := a$.

Since the generic constant c used in the above argument is independent of time, as long as all coefficient functions are bounded uniformly in time, this local solution can be extended to the hole time interval $[0,T]$. To this end, we consider a sequence of time intervals of equal lengths:

$$[t_0 = 0, t_1], \ldots, [t_{l-1}, t_l], \ldots, [t_{m-1}, t_m = T], \quad t_l - t_{l-1} = h.$$

To each of these subintervals, we apply the above existence result, choosing h sufficiently small, and taking as initial value $a_l := u_2(t_l)$ on the interval $[t_l, t_{l+1}]$ the end value of the solution on the preceding interval $[t_{l-1}, t_l]$. For the first time interval, we use the initial value of $u_2(0)$ from (3.30) or (3.31). The solutions $u_2 \in C[t_l, t_{l+1}]$ from the respective time intervals $[t_l, t_{l+1}]$ can then be used to construct the global solution $u_2 \in W(0,T)$. Having constructed u_2, we obtain from Lemma 3.6 the solution components u_0 and $u_1 \in W(0,T)$ and further $u_3, u_4, u_5, u_6, u_7 \in C^1[0,T]$. This proves the existence of a unique global solution of the system (3.24) - (3.35), which depends continuously (even Lipschitz continuously) on the initial data.

3.4 Proof of non-negativity

(i) *An auxiliary result:* We will use the following non-negativity result, which is an extension of Lemma 3.6 for the case of non-negative initial and boundary data. Usually such results are derived from maximum principles which are standard for Dirichlet boundary conditions. However, for the case of Neumann or Robin boundary conditions, other more subtle arguments have to be used (see, e.g., Ladyženskaja et al. [15]). Here, we provide an alternative proof by rather elementary arguments based on discretization such as already used in the proof of Theorem 3.1 for ODEs. Again, as a byproduct, we obtain a corresponding result for a discretized version of (3.56).

Lemma 3.7. *Suppose that additionally to the assumptions of Lemma 3.6 there holds* $g \geq 0$ *and* $v^0 \geq 0$. *Then, the corresponding unique solution* $v \in W(0,T)$ *also satisfies* $v \geq 0$ *on* $\overline{Q}_T := [0,T] \times \overline{\Omega}$.

Proof. The proof employs finite difference discretization in space and time, the inverse monotonicity of M-matrices (as already used in the proof of Theorem 3.1), and uniform convergence properties towards continuous limits.

For discretizing the initial-boundary value problem (3.56), we use the Shortley-Weller scheme in space (see Shortley & Weller [22] for the definition of this difference approximation and for its error analysis, e. g., Forsythe & Wasow [11], Bramble & Hubbard [5] and Hackbusch [12]) combined with the backward Euler scheme (3.19) in time. To this end, we cover the computational domain $\overline{\Omega}$ by a uniform cartesian grid of width h and the time interval $I = [0,T]$ by a uniform grid of width k. The set of "interior" spatial grid points (i. e., those contained in Ω) is denoted by Ω_h, while the intersections of the grid lines with the boundary $\partial\Omega$ form the set $\partial\Omega_h$ of "boundary" grid points. We set $\overline{\Omega}_h := \Omega_h \cup \partial\Omega_h$. Further, we denote by Ω_h^0 the set of all interior grid points for which all next neighbors in distance h are either also interior grid points or lie on the boundary $\partial\Omega$. At grid points in Ω_h^0 the Laplacian operator is discretized by the usual second-order central differences

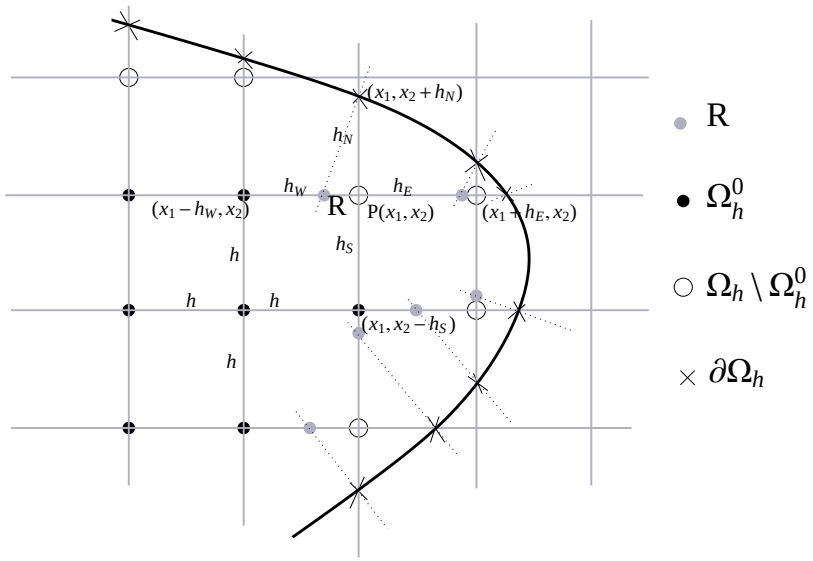

Figure 1. Sketch of Shortley-Weller discretization and of the discretization of Robin boundary conditions in 2D.

("3-point stencil in 1D, "5-point stencil" in 2D and "7-point stencil" in 3D), while at grid points in $\Omega_h \setminus \Omega_h^0$ the so-called Shortley-Weller modification is used as indicated in Fig. 1. At grid points in $\partial\Omega_h$ the Robin boundary condition is discretized by first-order backward differences, in 2D and 3D combined with linear interpolation between neighboring interior grid points as indicated in Fig. 1. A close examination of this difference approximation shows that the corresponding system matrix A_h for the grid variables $v_h(t) = (v_h(t,P))_{P\in\overline{\Omega}_h}$ is of non-negative type and diagonally dominant in the sense of Lemma 3.2. The Shortley-Weller-Scheme for a point near the boundary, $(x_1, x_2) \in \Omega_h \setminus \Omega_h^0$, reads as follows:

$$\begin{aligned} SWv_h(t,x_1,x_2) := D\Big\{ &-\frac{2}{h_N(h_S+h_N)}v_h(t,x_1,x_2+h_N) \\ &-\frac{2}{h_W(h_E+h_W)}v_h(t,x_1-h_W,x_2)+\Big(\frac{2}{h_E h_W}+\frac{2}{h_S h_N}\Big)v_h(t,x_1,x_2) \\ &-\frac{2}{h_E(h_E+h_W)}v_h(t,x_1+h_E,x_2)-\frac{2}{h_S(h_S+h_N)}v_h(t,x_1,x_2-h_S)\Big\}. \end{aligned} \tag{3.77}$$

The resulting matrix of this scheme is again of non-negative type and diagonally dominant. For a boundary point $(x_1, x_2) \in \partial\Omega_h$ we have

$$d(t) = \begin{pmatrix} \frac{r_{\text{act}}\text{pJAK}(t)}{|\partial\Omega_{\text{cyt}}|} + \frac{r_{\text{imp}}}{|\partial\Omega_{\text{nuc}}|} & 0 \\ -\frac{r_{\text{act}}\text{pJAK(t)}}{|\partial\Omega_{\text{cyt}}|} & \frac{r_{\text{imp2}}}{|\partial\Omega_{\text{nuc}}|} \end{pmatrix}$$

and the discretized Robin boundary condition looks as follows:

$$D\frac{v_h(t,x_1,x_2)-v_h(t,R)}{h_n} + d(t)v_h(t,x_1,x_2) = g_h(t,x_1,x_2),$$

where h_n is the distance in negative normal direction of the boundary point (x_1, x_2) to the nearest grid line (in 2D) or grid plane (in 3D) with cutting point R. For the unknown $v_h(t,R)$, we use a linear interpolation of the neighbouring points, where we have to take into account two situations, the interpolation along x_1- and x_2-direction:

$$v_h(t,R) = \frac{h_E v_h(t, x_1 - h_W, x_2 - h_N) + h_W v_h(t, x_1 + h_E, x_2 - h_N)}{h_E + h_W},$$

$$v_h(t,R) = \frac{h_S v_h(t, x_1 - h_E, x_2 + h_N) + h_N v_h(t, x_1 - h_E, x_2 - h_S)}{h_N + h_S}.$$

The final scheme for a boundary point $(x_1, x_2) \in \partial\Omega_h$ then reads

$$\begin{aligned} -\frac{Dh_E}{h_n(h_E + h_W)} v_h(t, x_1 - h_W, x_2 - h_N) + \Big(\frac{D}{h_n} I_2 + d(t)\Big) v_h(t, x_1, x_2) \\ - \frac{Dh_W}{h_n(h_E + h_W)} v_h(t, x_1 + h_E, x_2 - h_N) = g_h(t, x_1, x_2) \end{aligned} \tag{3.78}$$

or

$$\begin{aligned} -\frac{Dh_S}{h_n(h_N + h_S)} v_h(t, x_1 - h_E, x_2 + h_N) + \Big(\frac{D}{h_n} + d(t)\Big) v_h(t, x_1, x_2) \\ - \frac{Dh_N}{h_n(h_N + h_S)} v_h(t, x_1 - h_E, x_2 - h_S) = g_h(t, x_1, x_2). \end{aligned} \tag{3.79}$$

The resulting matrix of this scheme is also weakly diagonal dominant and of non-negative type. For all interior points we use the 5-point stencil operator which shows the same properties.

The linear system of ODEs resulting from this spatial semidiscretization has the form

$$v_h'(t) + A_h(t) v_h(t) = b_h(t), \;\; t \geq 0, \quad v_h(0) = (v^0(P))_{P \in \overline{\Omega}_h}, \tag{3.80}$$

with right-hand side $b_h(t) = (b_P(t))_{P \in \overline{\Omega}_h}$,

$$b_P(t) := \begin{cases} 0, & P \in \Omega_h, \\ g(t,P), & P \in \partial\Omega_h, \end{cases}$$

and with a matrix A_h being non-negative and diagonal dominant. Then, the discretization in time is by the standard backward Euler scheme resulting in the following sequence of linear systems:

$$(I_h + kA_h(t_m)) V_{h,k}^m = V_{h,k}^{m-1} + k b_h(t_m), \;\; m \geq 1, \quad V_{h,k}^0 = v_h(0). \tag{3.81}$$

For this space-time discretization there holds the following a priori error estimate (for the argument see, e. g., Hackbusch [12])

$$\max_{(t_m,P) \in \overline{Q}_T} \|V_{h,k}^m(P) - v(t_m,P)\| \leq c(u,T)\{k + h^2\}, \tag{3.82}$$

where $c(u,T) := c(T)\{\|\mathrm{D}_t^2 v\|_{L^\infty(Q_T)} + \max_{m=3,4} \|\nabla^m v\|_{L^\infty(Q_T)}\}$. Simple convergence

$$\max_{(t_m,P) \in \overline{Q}_T} \|V_{h,k}^m(P) - v(t_m,P)\| \to 0 \quad (h,k \to 0)$$

holds true under the weaker assumption that $D_t v, \nabla^2 v \in C(\overline{Q}_T)$. Hence, by Lemma 3.2 the matrix $I_h + kA_h$ is invertible with elementwise positive inverse $(I_h + kA_h)^{-1} > 0$. Since by assumption $V_{h,k}^0 \geq 0$, $b_h(t_m) \geq 0$, we conclude that $V_{h,k}^m \geq 0$ for all $m \geq 0$. Hence, by the convergence property (3.82) it follows that $v \geq 0$ on $\overline{Q}_T$. □

(ii) *The non-negativity result:* We recall the fixed-point iteration (3.76) on the time intervals $[t_l, t_{l+1}]$ defined in the preceding section. Suppose that the initial values $u_0(t_l), \ldots, u_7(t_l)$, are non-negative and that the starting value u_2^0 of the fixed-point iteration $u_2^{k+1} = \chi(u_2^k)$ on $[t_l, t_{l+1}]$ satisfies $u_2^0 \geq 0$, on $[t_l, t_{l+1}]$. Then, if $u_2^k \geq 0$, by the result of Lemma 3.7 the next iterate satisfies $u_0^{k+1} \geq 0$. Using this result in the boundary conditions (3.53) and (3.54), we obtain analogously that also $u_1^{k+1} \geq 0$. The other unkowns $\tilde{u} := \{u_2^{k+1}, \ldots, u_7^{k+1}\}$ are then determined by an ODE system of the form

$$v_{\text{nuc}} \tilde{u}'(t) + \tilde{A}(t)\tilde{u}(t) = \tilde{b}(t), \tag{3.83}$$

with the matrix

$$\tilde{A}(t) = \begin{bmatrix} r_{\text{exp}} & 0 & 0 & 0 & 0 & -r_{\text{delay}} \\ 0 & r_{\text{delay}} & 0 & 0 & 0 & 0 \\ 0 & -r_{\text{delay}} & r_{\text{delay}} & 0 & 0 & 0 \\ 0 & 0 & -r_{\text{delay}} & r_{\text{delay}} & 0 & 0 \\ 0 & 0 & 0 & -r_{\text{delay}} & r_{\text{delay}} & 0 \\ 0 & 0 & 0 & 0 & -r_{\text{delay}} & r_{\text{delay}} \end{bmatrix},$$

and the right-hand-side vector

$$\tilde{b}(t) = \begin{bmatrix} \frac{r_{\text{imp}}}{|\partial\Omega_{\text{nuc}}|} \int\limits_{\partial\Omega_{\text{nuc}}} u_0^k(t,x)\, do_x \\ \frac{r_{\text{imp2}}}{|\partial\Omega_{\text{nuc}}|} \int\limits_{\partial\Omega_{\text{nuc}}} u_1^k(t,x)\, do_x \\ 0 \\ 0 \\ 0 \\ 0 \end{bmatrix}.$$

The matrix $\tilde{A}(t)^T$ is of non-negative typ and diagonally dominant. Further, the initial values $\tilde{u}(0)$ and the right-hand side $\tilde{b}$ are non-negative. Hence, by Lemma 3.2 it follows that $\tilde{u} \geq 0$. In particular, there holds $u_2^{k+1} \geq 0$. Repeating this argument for the whole iteration $u_2^{k+1} = \chi(u_2^k)$, we obtain that in the limit $u(t,x) \geq 0$ for $(t,x) \in [t_l, t_{l+1}] \times \overline{\Omega}$. This eventually implies that $u \geq 0$ on the whole time interval $[0, \infty)$.

Remark 3.8. As a byproduct of the above argument, we see that the space-time discretization of the PDE-ODE system (3.24) - (3.35) by the second-order Shortley-Weller finite difference approximation in space and the first-order backward Euler scheme in time yields non-negative approximations $U_{h,k}^m \geq 0$ at all discrete time levels $t_m \geq 0$, and there holds the error estimate

$$\max_{(t_m, P) \in \overline{Q}_T} \|U_{h,k}^m(P) - u(t_m, P)\| \leq c(T)\{k + h^2\}, \tag{3.84}$$

provided that the solution is sufficiently regular. This shows that problem (3.24) - (3.35) can be numerically approximated. Analogous results hold true for any space-time discretization, which yields system matrices of M-matrix type. In the computations described in Section 4, below, we have used a low-order finite element discretization in space with piecewise (isoparametric) bi/tri-linear shape functions and the first-order backward Euler scheme in time. This combined space-time discretization does not satisfy the M-matrix requirement on general meshes but converges with the above order. However, in our computations, we have not observed any problems with the required non-negativity of the discrete solution.

3.5 Proof of boundedness and Lyapunov stability

(i) *Boundedness of solution:* From the conservation property of the quantity $\sigma := D^{-1}|\Omega|(\bar{u}_0 + \bar{u}_1) + v_{\text{nuc}}(u_2 + u_3 + u_4 + u_5 + u_6 + u_7)$ and the non-negativity of the solution u, we obtain

$$\sup_{t\in[0,\infty)} \max\{\bar{u}_0(t), \bar{u}_1(t), u_2(t), \ldots, u_7(t)\} < \infty.$$

Then, from the variational form of the equations (3.24) and (3.25),

$$\begin{aligned}(\partial_t u_0, \varphi)_\Omega + D(\nabla u_0, \nabla\varphi)_\Omega + \frac{r_{\text{imp}}}{o_{\text{nuc}}}(u_0, \varphi)_{\partial\Omega_{\text{nuc}}} \\ + \frac{r_{\text{act}}}{o_{\text{cyt}}}\text{pJAK}(t)(u_0, \varphi)_{\partial\Omega_{\text{cyt}}} = \frac{r_{\text{exp}}}{o_{\text{nuc}}}(u_2, \varphi)_{\partial\Omega_{\text{nuc}}},\end{aligned} \tag{3.85}$$

and

$$(\partial_t u_1, \varphi)_\Omega + D(\nabla u_1, \nabla\varphi)_\Omega + \frac{r_{\text{imp2}}}{o_{\text{nuc}}}(u_1, \varphi)_{\partial\Omega_{\text{nuc}}} = \frac{r_{\text{act}}}{o_{\text{cyt}}}\text{pJAK}(t)(u_0, \varphi)_{\partial\Omega_{\text{cyt}}}, \tag{3.86}$$

for $\varphi \in V$, we conclude that also

$$\sup_{t\in[0,\infty)} \{\|u_0\|_\Omega + \|u_1\|_\Omega\} < \infty. \tag{3.87}$$

To see this, we choose $\varphi = u_0$ in (3.85) and $\varphi = u_1$ in (3.86), to obtain

$$\begin{aligned}\frac{1}{2}\frac{d}{dt}\|u_0\|_\Omega^2 + D\|\nabla u_0\|_\Omega^2 + \frac{r_{\text{imp}}}{o_{\text{nuc}}}\|u_0\|_{\partial\Omega_{\text{nuc}}}^2 \\ + \frac{r_{\text{act}}}{o_{\text{cyt}}}\text{pJAK(t)}\|u_0\|_{\partial\Omega_{\text{cyt}}}^2 = \frac{r_{\text{exp}}}{o_{\text{nuc}}}(u_2, u_0)_{\partial\Omega_{\text{nuc}}},\end{aligned} \tag{3.88}$$

and

$$\frac{1}{2}\frac{d}{dt}\|u_1\|_\Omega^2 + D\|\nabla u_1\|_\Omega^2 + \frac{r_{\text{imp2}}}{o_{\text{nuc}}}\|u_1\|_{\partial\Omega_{\text{nuc}}}^2 = \frac{r_{\text{act}}}{o_{\text{cyt}}}\text{pJAK(t)}(u_0, u_1)_{\partial\Omega_{\text{cyt}}}. \tag{3.89}$$

From (3.88), we infer by standard arguments using the generalized Poincaré inequality

$$\|u_0\|_\Omega \le c\{\|\nabla u_0\|_\Omega + \|u_0\|_{\partial\Omega_{\text{nuc}}}\}, \tag{3.90}$$

and Young's inequality that

$$\frac{d}{dt}\|u_0\|_\Omega^2 + \lambda\|u_0\|_\Omega^2 + \gamma\{\|\nabla u_0\|_\Omega^2 + \|u_0\|_{\partial\Omega_{\text{nuc}}}^2\} \le c\|u_2\|_{\partial\Omega_{\text{nuc}}}^2,$$

with certain data-dependent constants $\lambda, \gamma, c > 0$. From this, we conclude

$$\frac{d}{dt}\Big(e^{\lambda t}\|u_0\|_\Omega^2\Big) + \gamma e^{\lambda t}\{\|\nabla u_0\|_\Omega^2 + \|u_0\|_{\partial\Omega_{\rm nuc}}^2\} \le c e^{\lambda t}\|u_2\|_{\partial\Omega_{\rm nuc}}^2,$$

and integrating this with respect to time,

$$\|u_0(t)\|_\Omega^2 + \gamma e^{-\lambda t}\int_0^t e^{\lambda s}\{\|\nabla u_0\|_\Omega^2 + \|u_0\|_{\partial\Omega_{\rm nuc}}^2\}\,ds \le c e^{-\lambda t}\int_0^t e^{-\lambda s}\|u_2\|_{\partial\Omega_{\rm nuc}}^2\,ds.$$

This yields

$$\begin{aligned}\sup_{[0,\infty)}\Big\{\|u_0\|_\Omega^2 + \gamma e^{-\lambda t}\int_0^t e^{\lambda s}\Big\{\|\nabla u_0\|_\Omega^2 + \|u_0\|_{\partial\Omega_{\rm nuc}}^2\Big\}\,ds \\ \le \|u_0(0)\|_\Omega^2 + c\lambda^{-1}\sup_{[0,\infty)}\|u_2\|_{\partial\Omega_{\rm nuc}}^2 < \infty.\end{aligned} \tag{3.91}$$

In the next step, we will use the estimate

$$\|u_0\|_{\partial\Omega_{\rm cyt}} \le c\|u_0\|_V \le c\{\|\nabla u_0\|_\Omega + \|u_0\|_{\partial\Omega_{\rm nuc}}\}, \tag{3.92}$$

which follows by a trace inequality and a generalized Poincare inequality (3.90). Then, from (3.89), we infer using again Young's inequality and the Poincaré inequality (3.90) for u_1 that

$$\frac{d}{dt}\|u_1\|_\Omega^2 + \lambda\|u_1\|_\Omega^2 \le c\|u_0\|_{\partial\Omega_{\rm cyt}}^2.$$

From this, we conclude

$$\frac{d}{dt}\Big(e^{\lambda t}\|u_1\|_\Omega^2\Big) \le c e^{\lambda t}\|u_0\|_{\partial\Omega_{\rm cyt}}^2,$$

and integrating this with respect to time,

$$\|u_1(t)\|_\Omega^2 \le c e^{-\lambda t}\int_0^t e^{-\lambda s}\|u_0\|_{\partial\Omega_{\rm cyt}}^2\,ds.$$

In view of the estimates (3.91) and (3.92) it follows finally that

$$\sup_{[0,\infty)}\|u_1\|_\Omega^2 \le c\lambda^{-1}\sup_{[0,\infty)}\|u_2\|_{\partial\Omega_{\rm nuc}}^2 < \infty. \tag{3.93}$$

This completes the proof of the estimate (3.87).

(ii) *Lyapunov stability of solution:* Again, we recall the fixed-point iteration (3.76) on the time interval $[t_0, t_1]$ for $z(t,x)$ being the disturbed zero-solution with disturbed initial data z^*, satisfying $\|z^*\| < \delta(\varepsilon)$. The estimates (3.91) and (3.93) show that the solutions $z_0^{k+1}(t,x)$ and $z_1^{k+1}(t,x)$ can be bounded by its initial values z_0^*, z_1^* and $z_2^k(t)$, which is the first component of the autonomous nonhomogenous system (3.83). All other components of this system, z_i^{k+1}, $i = 3,4,5,6,7$, can also be bounded by $z_2^k(t)$ as already shown in the estimates (3.71) and (3.72). Further, we have

$$\|z_2^{k+1}\|_\infty^2 \le c(t_1 - t_0)\|z_2^k\|_\infty < \varepsilon,$$

with a suitable choice of δ. This argument can be extended to the hole time interval $[0,T]$ as already mentioned in the existence proof in Section 3.3. This shows the Lyapunov stability of the solution.

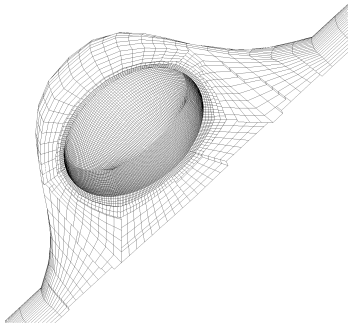

(a) shape of NIH-3T3 cell (b) recessed nucleus

Figure 2. Computational meshes (created with [2]) for the simulation of the NIH-3T3 cell (left) and zoom into the cell neighborhood of the nucleus (right).

4 Numerical Computations

In order to obtain numerical solutions of time courses to simulate our biological system, we used the in-house software package Gascoigne (available under [10]). This software tool uses a conforming finite element method (FEM) with (isoparametric) bi/tri-linear shape functions for spatial discretization and, among others, the backward Euler scheme for time discretization of the PDE model. For details of such a spatial discretization and the related notation, we refer to the standard textbook literature, e. g., Ciarlet [7] or Brenner & Scott [6]. The geometry and meshes used in our simulation are shown in Fig. 2.

One goal of this paper is to prove the well-posedness of the model as basis of a reliable simulations. Fig. 3 shows the time-dependent Robin boundary coefficient which was possible to measure in this case such that the signaling model could be simplified to a linear one. The results shown in Table 2 confirm that our numerical results are reliable in the sense that they are "converged", i. e., they do not change anymore under further mesh refinement. Some comparison results concerning the use of a pure ODE model and the enhanced PDE-ODE model for intracellular signaling are collected in Fig. 3 (b). We conclude that by considering diffusion of the molecules inside the cytoplasm their sojour time there is longer and, in turn, less molecules are available in the nucleus for binding to the DNA. The difference for pSTAT5 is here about $0.7\ \mathrm{mol}/\mu\mathrm{m}^3$. We observed a 11% gradient for the total STAT5 concentration. which corresponds to $1.5\ \mathrm{mol}/\mu\mathrm{m}^3$ (mol = molecules). The main concentration comes from the activated molecules, $pSTAT5$.

5 Conclusion

In this article, we present the mathematical treatment of a model of the JAK2/STAT5 signaling pathway, which consists of a coupled system of linear differential equations (PDEs + ODEs) involving high-quality quantitative data from our experimental collaborators. This model is formulated to analyze the effect of cellular geometries on signaling, i.e., pro-

mesh level	# nodes	$\bar{u}_{1,h}(5)$	$\bar{u}_{1,h}(16)$	$\bar{u}_{1,h}(155)$
0	24 150	2.09198	2.40505	1.80197
1	51 354	2.09279	2.4042	1.80189
2	160 158	2.093	2.40399	1.80186

Table 2. Convergence results for the functional of interest $\bar{u}_1$ at different time instants.

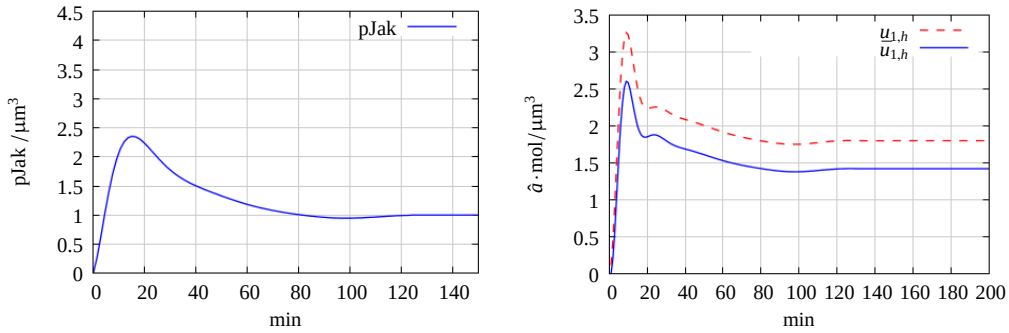

(a) pJak(t) of NIH-3T3 cell

(b) space averaged solution on the finest mesh via the PDE-ODE model (red) and via the pure ODE model (blue)

Figure 3. Timecourse of the parameter *pJak* entering in the Robin boundary condition (left) and comparison of the solutions $\bar{u}_{1,h}(t) = \int_\Omega u_1(t,x)dx$ from the PDE model with $u_1(t)$ from the ODE model (right).

cesses important for the transport inside the cytoplasm are modeled in detail, while other processes like the receptor-model or processes taking place in the nucleus (DNA-binding, dephosphotylation, ...) are simplified due to measured data or by delay-equations. Firstly, the ODE model is analyzed to show its well-posedness, i.e., the existence, uniqueness, non-negativity, boundedness, asymptotics and stability of the solution. Then, analogous results are proven for the more realistic, yet linear, PDE-ODE model. The mathematical techniques used are chosen in such a way that they apply to the continuous model but also to a suitably discretized version and prepare also for an analysis of more general nonlinear models coming from signaling processes.

Acknowledgments

This work was supported by the Helmholtz Alliance on Systems Biology (SBCancer, Submodule V.7).

Special thanks to PD Dr. U. Klingmüller, Division Systems Biology of Signal Transduction, DKFZ-ZMBH Alliance, German Cancer Research Center, Im Neuenheimer Feld 280, 69120 Heidelberg, Germany and in particular to Dr. Andrea C. Pfeifer.

References

[1] Adams, R. A., Fournier, J. J. F., *Sobolev spaces*, Elsevier, 2003.

[2] *ANSYS ICEM CFD Mesh Generation*, URL: http://www.ansys.com/-products/icemcfd.asp.

[3] Bachmann, J., Dynamic Modeling of the JAK2/STAT5 Signal Transduction Pathway to Dissect the Specific Roles of Negative Feedback Regulators, dissertation, University of Heidelberg, 2009.

[4] Bermon A., and Plemmons R. J., *Nonnegative Matrices in the Mathematical Sciences*, SIAM Publication, Philadelphia, 1994.

[5] Bramble J. H., and Hubbard B. E., *Approximation of Solutions of Mixed Boundary Value Problems for Poisson's Equation by Finite Differences*, J. ACM 12, 114-123, DOI=10.1145/321250.321260 http://doi.acm.org/10.1145/321250.321260, 1965.

[6] Brenner S. C., and Scott R. L., *The Mathematical Theory of Finite Element Methods*, Springer, Berlin-Heidelberg-New York, 1994.

[7] Ciarlet P. G., *Introduction to Numerical Linear Algebra and Optimization*, Cambridge University Press, Cambridge, UK, 1988.

[8] Claus J., Friedmann E., Klingmüller U., Rannacher R., and Szekeres T., *Spatial aspects in the SMAD signaling pathway*, J. Math. Biol., DOI 10.1007/s00285-012-0574-1, 2012.

[9] Friedmann E., Pfeifer A.C., Neumann R., Klingmüller U. and Rannacher R., *Interaction between experiment, modeling and simulation of spatial aspects in the JAK2/STAT5 Signaling pathway*, in Model based parameter estimation: theory and applications, Springer Series Contributions in Mathematical and Computational Sciences, 2011.

[10] GASCOIGNE, *High Performance Adaptive Finite Element Toolkit*, URL: `http://www.numerik.uni-kiel.de/~mabr/gascoigne/`.

[11] Forsythe G. E., and Wasow W. R., *Finite-difference Methods for Partial Differential Equations*, John Wiley, New York, 1960.

[12] Hackbusch W., *Elliptic Differential Equations: Theory and Numerical Treatment*, Springer, Berlin, 1992.

[13] Hairer E., Norsett S. P., and Wanner G., *Solving Ordinary Differential Equations I: Nonstiff Problems*, Springer, Berlin-Heidelkberg-New York, 1987.

[14] Jost J., *Partial Differential Equations*, Springer, 2007.

[15] Ladyženskaja O. A., Solonnikov V. A., and Uralćeva N. N., *Linear and Quasilinears Equations of Parabolic Type*, American Mathematical Society, 1968.

[16] Liebermann G. M., *Second Order Parabolic Differential Equations*, World Scientific Publishing Co. Pte. Ltd, 1996.

[17] Maiwald T., and Timmer J., *Dynamical Modeling and Multi-experiment Fitting with PottersWhee*l, Bioinformatics 24, 2037-43, 2008.

[18] Neumann R., *Räumliche Aspekte in der Signaltransduktion, Diplomarbeit* Ruprecht-Karls- Universität Heidelberg, 2009.

[19] Pfeifer A.C, Kaschek D., Bachmann J., Klingmüller U., and Timmer J., *Model-based extension of high-throughput to high-content data*, 2008.

[20] Schilling M, Maiwald T, Bohl S, Kollmann M, Kreutz C, Timmer J, and Klingmüller U., *Computational processing and error reduction strategies for standardized quantitative data in biological networks*, FEBS J. 272(24):6400-11, 2005.

[21] Schilling M., Pfeifer A.C., Bohl S., and Klingmüller U., *Standardizing experimental protocols*, Curr Opin Biotechnol., 2008.

[22] Shortley G. H., Weller R., *Numerical Solution of Laplace's Equation*, J. Appl. Phys. 9, 334–348, 1938.

[23] Swameye I., Müller T.G., Timmer J., Sandra O., and Klingmüller. U., *Identification of nucleocytoplasmatic cycling as a remote sensor in cellular signaling by databased modeling*, PNAS Proceedings of the National Academy of Sciences, 100(3):10281033, 2003.

[24] Timmer J., Müller T.G., Swameye I., Sandra O., and Klingmüller U., *Modeling the nonlinear dynamics of cellular signal transduction*, International Journal of Bifurcation and Chaos, 14, No. 6, 2069-2079, 2004.

[25] Varga R. S., *Matrix Iterative Analysis*, Prentice-Hall, Englewood Cliffs, N. J., 1962.

[26] Wloka J., *Partial Differential Equations*, Cambridge University Press, 1987.